Battery Supported Electric Vehicle Charging Plaza Using a Limited Capacity Grid Connection

Edward Heath[1], Rick Wolburtus, Renée Heller

[1]*Author 1 (corresponding author) Amsterdam University of Applied Sciences, e.p.heath@hva.nl*

Executive Summary

This study used historical data from a Park & Ride facility in Amsterdam to build a validated computer (Python) model to optimize battery and grid connection sizing. The case study modelled is equipped with 8 EV chargers (16 connections), an on-site supplementary battery, and a limited capacity grid connection. This model was then used to optimize the battery energy storage capacity and grid connection capacity for minimal annualized investment, using a future proof monthly load profile. A variety of battery control strategies were simulated using both the optimal system sizing and the current system sizing. The results were compared and a recommended control strategy presented, considering a number of performance metrics.

1 Introduction

The city of Amsterdam, like many other regions in The Netherlands and further afield, is facing an increase in electrical power demand fuelled by clearly defined targets for the electrification of the transport and built environment sectors [1]. The city of Amsterdam has set out a target to be natural gas free by 2040 and to reduce CO2 emissions by 55 % before 2030, with 25 % of the CO^2 reductions coming from the built environment and 18 % from mobility [2].

The city and municipality have also imposed targets for the installation of public charging infrastructure, with approximately 31000 public and semi-public charge points required by 2030 to supply the predicted 250000 passenger cars and 23000 vans [3]. This will be equivalent to 1 charge point for every 15 parking spaces. Currently approximately 75% of the 9600 EV charge points are public or semi-public [3] due to the residential portfolio resulting in few privately owned houses with drive ways. Meanwhile, personal passenger electric vehicles (EVs) presently account for 6 % of the registered Dutch M1 fleet, a total of 31000 EVs, and electric busses account for 17% of the M2 & M3 bus fleet [4]. In Amsterdam,

Whilst the local and national distribution and transmission network operators are working to expand grid capacity, through upgraded and newly built transformer stations and more extensive cabling, this will of course take time. It is estimated that the necessary grid reinforcements will take several years, with new large user connections (defined as being greater than 3x80 A, 55.4 kW) estimated at taking 1.5 years, with more complex and isolated connections taking longer [5]. For small consumers (less than 3x80 A) a lead time of 18 weeks is the target [5]. Therefore, in order to maintain the security of supply innovative short-term solutions are required.

In a bid to further incentivize and provide for EVs whilst minimizing the grid impact, the city of Amsterdam, in partnership with local energy service provider Vattenfall and maintenance provider Heijmans, have installed a novel charging solution at a Park and Ride (P&R) facility. So as to be considered a small consumer, and therefore benefit from a faster connection time, a maximum grid connection capacity of 3x80 A was

imposed. This limited capacity grid connection necessitated the installation of a supplementary on-site battery to ensure security of supply and maintain user experience. Additionally, the lead time and costs of further increasing the grid connection capacity rise rapidly [6].

The system has been operational for 18 months at the time of writing this paper. In that time adequate usage data has been collected to develop a validated stochastic system model in Python, optimize the battery energy storage capacity and grid connection capacity for a future proof load profile of 7 MWh, and to test this optimal result with various battery control algorithms.

The motivation for this study is the oversized battery for current operation; in the three months used to build the model the battery dropped below 50 % SOC 9 times and the battery is cycled too frequently for low energies. Considering that the grid connection capacity could still further be increased from the programmed 3x25 A up to the physical connection of 3x80 A, which remains a cheaper option than the annualised battery system costs, the battery energy storage capacity could be reduced. Therefore, this study aims to answer the following research questions:

What is the minimal battery energy storage capacity and grid connection capacity that can suitably supply the monthly load demand now and in a potential future high demand month of 7 MWh?

How does this combination perform for a variety of battery control strategies?

1.1 The System

The main characteristics that define the battery system and charge points are presented in Tab. 1. There are 8 dual connection EV charge points, meaning 16 available connectors. Each dual connection charge point has had the phase connections rotated, as standard, and conventional load sharing is applied when necessary.

Table 1: System components

	Brand and Model	Specifications
Battery	BMW i3 cells	240 kW, 336 kWh
Charge points	Alphen Twin Public	3x35 A @ 400 V, 24.2 kW
		13.75 kW, 20 A per connector

2 Methodology

2.1 Data Filtering and Model Formation

Data in the months of April, May and June 2022 were used to build the model, with the month of July used to validate it. Individual charging events were identified and various session parameters determined, namely the day of week, entry time, exit time, end of charging time, power delivery per time step, number of phases connected to and the current per phase. From this the maximum charging power, total energy delivered, and connection and charging duration per charging event were deduced. Any vehicle that was charged for a long continuous period followed thereafter by blocks of ~5 min pulses were filtered such that only the initial, continuous, energy transfer was considered. This continuous charging period accounted for over 96 % of total energy transfer in these sessions. The charging sessions were then filtered for charging duration and energy transfer, with limits [0.5 hr, 25 hr) and [1 kWh, 80 kWh) respectively. Tab 2 shows the final values.

Distributions of start time per weekday, maximum charging power, connection duration, and energy demand could then formed from this charge session data, as well as the ratio of phase connections. The distribution of charge power is shown in Fig 1. Considering that the fuse current per connector is 20 A, it is clear that 1- and 3-phase vehicles are far more common.

Table 2: Initial user count and energy demand per month, after filtering

Month	User count	Total energy demand (kWh)	Mean energy per user (kWh)
April	182	4125	22.66
May	177	3528	19.93
June	213	4405	20.68
July	219	4785	21.85
Total	920	13843	21.28
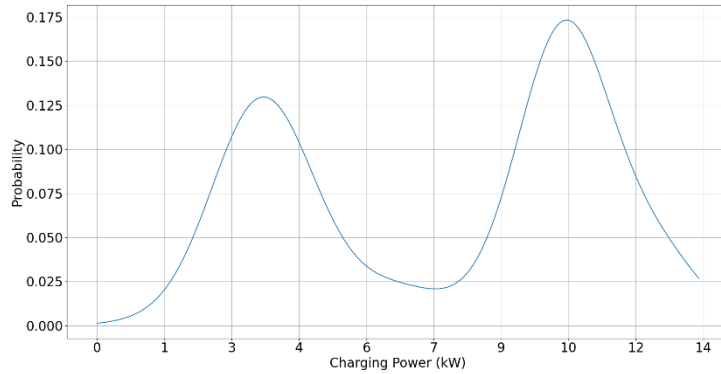
Figure 1: Charging power distribution from measured data

The charge sessions were then split based on their maximum charging power into charging power bands that approximate EV charging powers, considering that the charging power delivered was not always the maximum demanded. These power bands were (1 kW, 4.6 kW), [4.6 kW, 7.2 kW), [7.2 kW, 14 kW). Considering that different EVs have different battery capacities, phase connections, and charging powers, these user groups will inherently have different usage profiles. Therefore, a different energy demand distribution was formed for each of the charging power bandwidths.

The entry events were separated by day since Friday, Saturday, and Sunday experience different usage patterns than the working weekdays Monday – Thursday, as presented in Fig 2. This was to be expected since Monday – Thursday people generally follow similar work-life patterns. For many people in the Netherlands Friday is a no-work day and it appears many people arrive late on a Friday to then park for the weekend. Saturdays are a day in which people travel to the city for social/leisure purporses whilst Sunday may still be regarded as a day of rest and therefore reduced P&R activity.
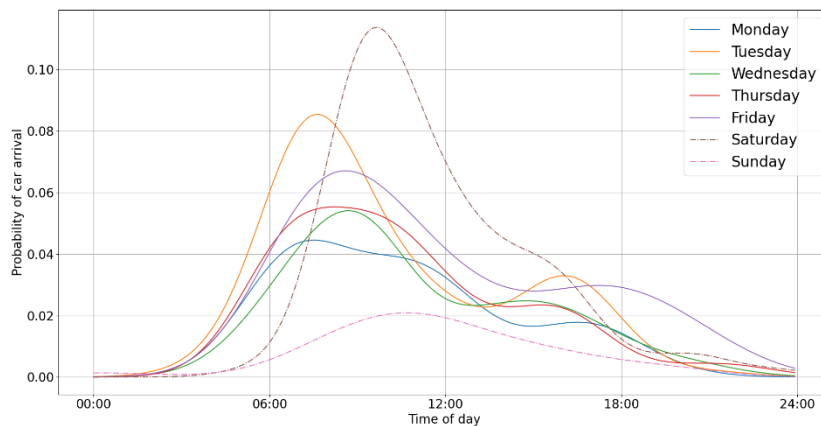

Figure 2: Probability density of car arrival at a given time per day of week. Weekends are notably different and Friday has a higher evening entry rate than the rest of the week

The model had a 5 minute resolution. At each time step, per day, an associated probability of car entry (with coefficient) is compared against a randomly generated number. Upon connection event, the number of phase connections is sampled from the distribution of measured data. Depending on the number of phases, the maximum charging current was sampled from the corresponding distribution. This distribution describes the maximum measured phase current per charge event from historical data. The charging power was then calculated and the energy demand was sampled from the respective power band distribution. In this model $V_{line-neutral}$ is assumed to be kept constant at 230 V.

$$P = N_{phases} \cdot I \cdot V_{line-neutral} \tag{1}$$

The connection duration was determined based on the time of entry, namely; before 10:00, between 10:00 and 16:00, and after 16:00, and the respective power distributions. Some noise (σ=0.025) was added to the charging power. A base load (system electronics, CP electronics), inverter idle power drain, and auxilliary load (battery aircon) were added. These were all sampled from distributions formed from historical data. If energy delivered in a charge session reached 75 kWh then the charge session ended early and the charge end time updated.

The power was delivered by either the grid, the battery, or a combination. In the case that load was less than the maximum grid capacity, any residual grid capacity would charge the battery. If the battery was empty, conventional load sharing of the available grid capacity was employed, ensuring base loads were also provided for. Thus, assuming base load was split evenly across the three phases, the power delivered to each EV at time t:

$$P_{EV,G,x}(t) = \frac{I_{Ph1,x}(t) + I_{Ph2,x}(t) + I_{Ph3,x}(t)}{I_{Ph1,T}(t) + I_{Ph2,T}(t) + I_{Ph3,T}(t)} \cdot (P_G(t) - P_{Base}(t)) \tag{2}$$

Where $P_G(t)$ is available power from the grid at time t and $P_{Base}(t)$ is the total base power at time t. The numerator consists of the current draw per phase for EV x at time t, and the denominator consists of the total current demand per phase at time t.

For battery charging and discharging, the inverter efficiency was sampled from the efficiency curve depicted in Fig 3. The curve was fitted to the filtered data using equation 3, and initial values a = 0.95, b = - 0.9, and c = 0.25.
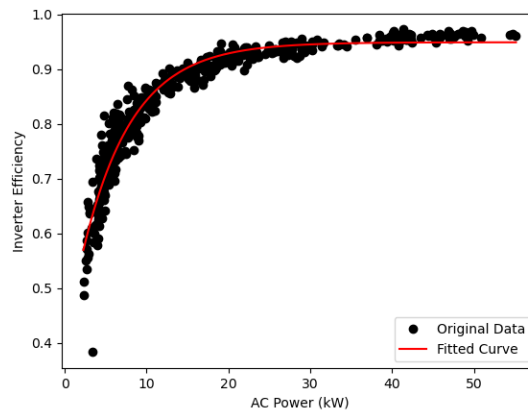
$$y = a + b \cdot e^{-c \cdot x} \tag{3}$$

Figure 3: Inverter efficiency vs AC side power

2.2 Model Validation

By comparing a 'base-case' simulation to July data the model was validated. The system usage in both the installed system and simulated base case are presented in Fig 4a and Fig 4b, respectively. The top plot depicts the power balance between grid import, battery and load, the middle plot shows the battery SOC, and the bottom plot shows the carpark occupancy and actively charging occupancy. The clearest difference is that the modelled battery control maintains the maximum SOC of 95% given the energy leakage over time. The installed system does not maintain the SOC in this way. Additionally, the simulated connection duration appears to be longer, although this has no impact on the system performance. There are available spaces and the majority of these vehicles are not charging, if it all. A direct comparison of the system metrics are presented in Tab 3.
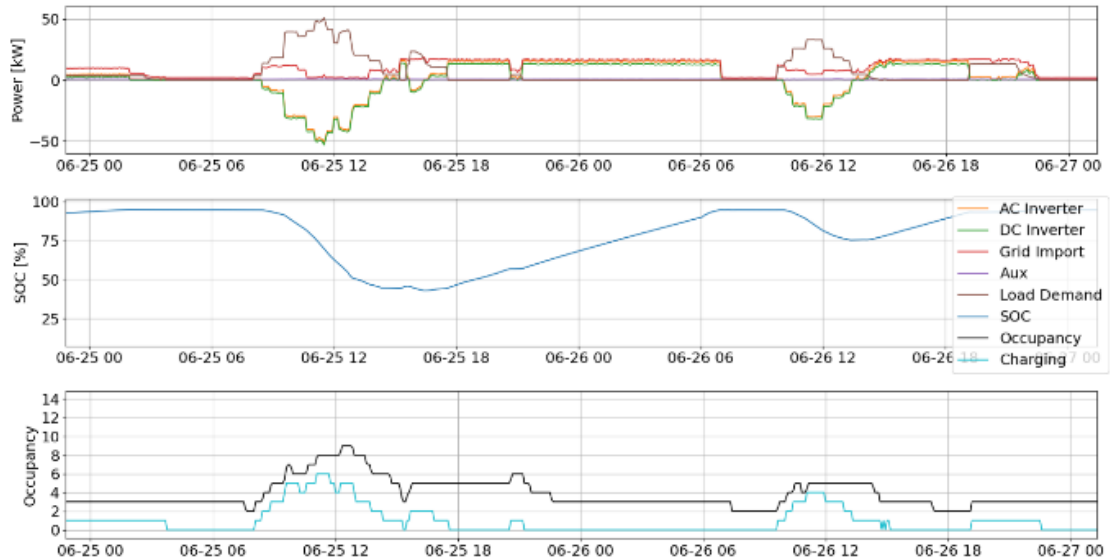

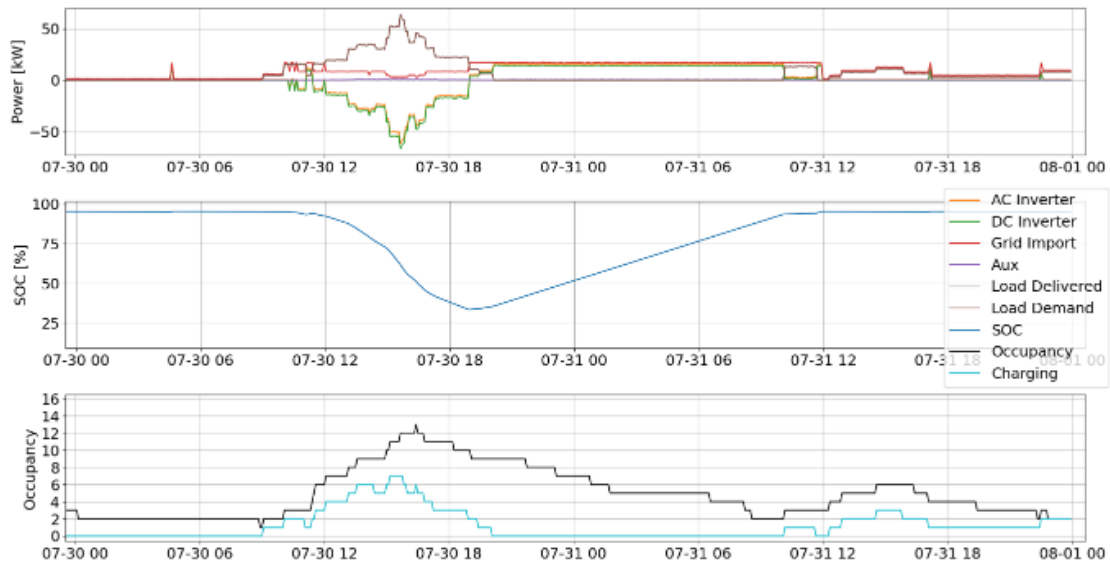Figure 4a: Typical usage of the P&R system for the measured data,

Figure 4b: Typical usage of the P&R system for the simulated base case.

Table 3: Performance metrics of measured data from the installed system and the simulated base case

	Measured Data	Simulated Base Case
Total load demand [kWh]	4785	4895
Number of charge events	219	244
Mean energy per charge event [kWh]	21.80	20.05
Mean charging power [kW]	7.79	7.65
Mean connection duration [hours]	13.00	13.28
Mean charging duration [hours]	3.46	3.09

The fit of the model is in line with the measured data. The slight reduction in mean charging duration observed in the model is a result of users that leave prior to fully charging their allotted energy demand. The energy demand assigned to each charge session is sampled from the distribution of measured energy delivered.

The measured battery system round-trip efficiency was found to be 72.0 % and was influenced by the battery energy efficiency of 95.6 % and the inverter efficiency for charging and discharging, as depicted in Fig 3, with mean values of 71.8 % and 88.6 %. Bear in mind, the mean efficiency values are not representative of energy transfer.

Table 4: Load and delivered battery powers from measured data

	Maximum	Mean
Load power	56.1 kW AC	12.9 kW AC
Battery power (charging)	17.3 kW AC	10.6 kW AC
Battery power (discharging)	55.1 kW AC	15.1 kW AC

One aspect that proved difficult to model was the grid contribution to load demand during battery discharge. The expectation was that it depended either on magnitude of load demand or phase balancing, and although there was some correlation between the phase current balance and grid contribution, it was not clear nor comprehensive. Thus, an approximation that resemebled observation was implemented, following magnitude of load demand.

2.3   Optimisation Problem

Regularly experiencing discharge cyles to a SOC of no less than 75 % and with the possibility to further increase the grid connection capacity, the battery was deemed too large for the currently observed usage. To this end, this study optimised both the battery energy storage capacity and the grid connection capacity for a future proof monthly load profile of 7 MWh (28 kWh/CP/day). This was deemed suitable since the maximum observed monthly load since installation was 6.1 MWh (24 kWh/CP/day). The Pymoo Python library [7] was used to form and solve the optimisation problem using a $(\mu+\lambda)$ genetic algorithm. This library was chosen for its ease of use and high quality documentation.

The objective function is presented in equation 4:

$$\min f(x) = \frac{C_B \cdot E_{B,max}}{L_{exp}} + C_G + 12 \cdot C_S \cdot \frac{LL}{\eta_S} \tag{4}$$

Where C_B is the cost of battery system installation, 250 €/kWh [8]. C_G is the cost of installation per grid connection capacity as presented in equation 5 [6]. C_S is the profit from electricity sale, 0.1 €/kWh. The battery investment is anuallised by dividing by the expected system lifetime L_{exp}, 10 years as per the supplier capacity waranty. Similarly, the monthly loss of load is annualised by multiplying by 12.

$$C_G(P_G) = \begin{cases} 346 \ \text{€/year}, & P_G = 3x25 \ A \\ 1459 \ \text{€/year}, & P_G = 3x35 \ A \\ 2148 \ \text{€/year}, & P_G = 3x50 \ A \\ 3533 \ \text{€/year}, & P_G = 3x80 \ A \end{cases} \qquad (5)$$

To maintain the battery power-energy ratio, in the installed system observed to be 0.71, constraint 6 was implemented. This allowed for some margin around the fixed value. To ensure the system is not massively undersized, constraint 7 was implemented limiting the lost potential load, *LL*.

$$0.7 \cdot E_{B,max} \leq P_{B,max} \leq 0.75 \cdot E_{B,max} \qquad (6)$$

$$LL = \sum_{t_0}^{T} \frac{P_{EV,D}(t) - P_G(t) + P_B(t) - P_{Base}(t)}{t_i} \leq 100 \qquad (7)$$

Where $P_{EV,D}(t)$ is the total EV power demand at time t, $P_G(t)$ is the power supplied by the grid at time t, $P_B(t)$ is the power supplied by the battery at time t, and $P_{Base}(t)$ is the base load at time t. The battery current convention employed is a negative battery power for discharging. t_i is the incremental 5 minute time step and T is the total time period of 1 month. All other constraints, 8 - 11, were internal to the system model and were handled during simulation runtime. These included the power balancing, the battery SOC limits, and the battery charge/discharge power limits.

$$P_{Base}(t) + P_{EV,D}(t) + P_B(t) = P_B(t) + P_G(t), \qquad \forall t \in T \qquad (8)$$

$$0.10 \cdot E_{B,max} < E_B(t) < 0.95 \cdot E_{B,max} \qquad (9)$$

$$0 \leq P_{B,ch,t} \leq P_{B,ch,max} \qquad (10)$$

$$0 \leq P_{B,dch,t} \leq P_{B,dch,max} \qquad (11)$$

Due to the stochastic nature of the model a single month-long load profile was formed and repeatedly used for the iterative optimization process, as described below:

1. A parent population of the variables $E_{B,max}, P_{B,max}, I_{G,max}$ was selected
2. The simulation was performed and the outputs LL and η_S were retrieved
3. Using these five decision variables the objective function was evaluated and the results saved
4. A new parent population was created as the GA describes, allowing for crossover and mutation

2.4 Control Strategies Investigated

The installed system round trip efficiency was identified to be underperforming. This was primarily due to the conversion losses at low charging and discharging powers of the supplementary battery. Additionally, the battery made frequent and small discharge/charge cycles, thus decreasing the battery lifetime [9, 10] and there was no consideration for power draw from the grid during peak hours. Given the current state of the power grid it is logical to limit the power draw from the grid during the peak demand hours of approximately 17:00 to 20:00. The following control scenarios were therefore decided upon:

1. Base case in which the grid supplies all load up the maximum capacity. When the battery starts discharging, at load powers above the maximum grid capacity, the grid contribution is reduced.
2. Limited peak hour power draw control is the same as the base case but during the peak grid load hours of 17:00 – 20:00 all load is supplied by the battery. If there is no EV load or the battery is depleted the grid will only supply the base load.
3. Minimum required battery charging and discharging power of 10 kW and 15 kW. If the EV load is above this deadband the battery supplies the entire load.

4. The combination of limited peak hour power draw and minimum required battery charge/discharge power of both 10 kW and 15 kW.

Each scenario was simulated using the future proof optimal sizing determined in section 2.3 and compared against the current system sizing. Due to the randomness inherent in the stochastic model, each scenario was simulated 5 times and averaged. The chosen performance metrics were:

- System round trip efficiency (η_S)
- Potential load not delivered (lost load, LL)
- Energy drawn from the grid during peak hours (E_{PH})
- Total load met by battery (L_{BT})
- Number of users that were still charging when they disconnected (N)

3 Results & Discussion

3.1 Optimal System Sizing

With the use of a genetic algorithm it was possible to determine the optimal battery energy storage capacity and grid connection capacity for a future proof monthly load profile of 7 MWh. The problem considered the base case battery control method and the discrete grid connection capacities, namely 3x25 A, 3x35 A, 3x50 A, and 3x80 A. The algorithm used a population size of 40 for 10 generations.

For the monthly load profile of 6874 kWh, which approximated the intended 7 MWh profile, the optimal results presented in Tab 5 were deduced. This is listed alongside the current installed system sizing for which a simulation using the exact same load profile was performed, resulting in the higher monthly lost load and higher annual cost. Furthermore, the pricing calculations used here are composed of values found in literature rather than the actual cost of installation which are somewhat higher for a pilot project like this.

Table 5: Optimal system sizing compared to installed system

	Installed System	Optimal System
Grid connection capacity, I_G	3x25 A	3x80 A
Battery energy storage capacity, E_B	336 kWh	143 kWh
Battery power capability, P_B	240 kW	103 kW
Annualised investment	€9857 / year	€7118 / year
Loss of potential load, LL	705 kWh	7 kWh

3.2 Comparative Analysis of Optimal and Current System Sizing

The optimal system sizing present in section 3.1 was used with a variety of control strategies, described in section 2.4, for a monthly load profile of 5 MWh. These were then compared against the current system sizing settings for the same scenarios. The abbreviations *BR* and *PHBR* refer to control strategies Battery Requirement and Peak Hour Battery Requirement, respectively.

Fig 5 shows the loss of potential load in each control scenario. In every control strategy the optimal settings performed better than the current settings. All battery control strategies that imposed a battery charge/discharge requirement experienced a higher loss of potential load than the respective base case. Interestingly, for the optimal settings, the 15 kW PHBR strategy had a lower loss of load than the 10 kW PHBR strategy. A 10 kW discharge power requirement would see the battery more regularly discharging and therefore more often at a lower SOC come peak grid load hours than with a 15 kW discharge requirement.
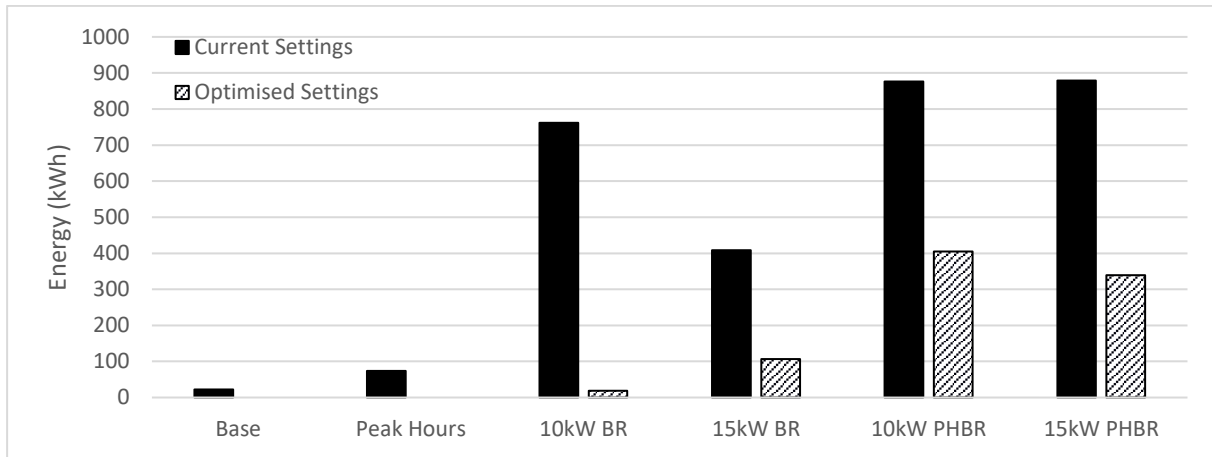
Figure 5: Potential load not supplied

The battery system round trip efficiency is increased for all control scenarios when the optimal settings are used, as depicted in Fig 6, when compared to current settings. This is due to the increased grid connection capacity that can charge the battery at high powers and also results in the battery only discharging at high powers. A higher charging/discharging battery power has a higher conversion efficiency in the inverter, as observed in Fig 3.

It can also be deduced that imposing the battery charging/discharging power requirement increases battery round trip efficiency. However, with optimised settings, all scenarios that limited peak hour grid import saw a reduced efficiency with respect to the base case. During peak grid load hours the battery control is altered to supply any EV load demand since the grid cannot. When considering the high grid connection capacity would supply all load powers up to 55 kW during regular hours, the battery which would otherwise supply a minimum of 43 kW (due to the shared battery and grid contribution to load supply during battery discharge) then discharges at lower powers and reduces the system round-trip efficiency.
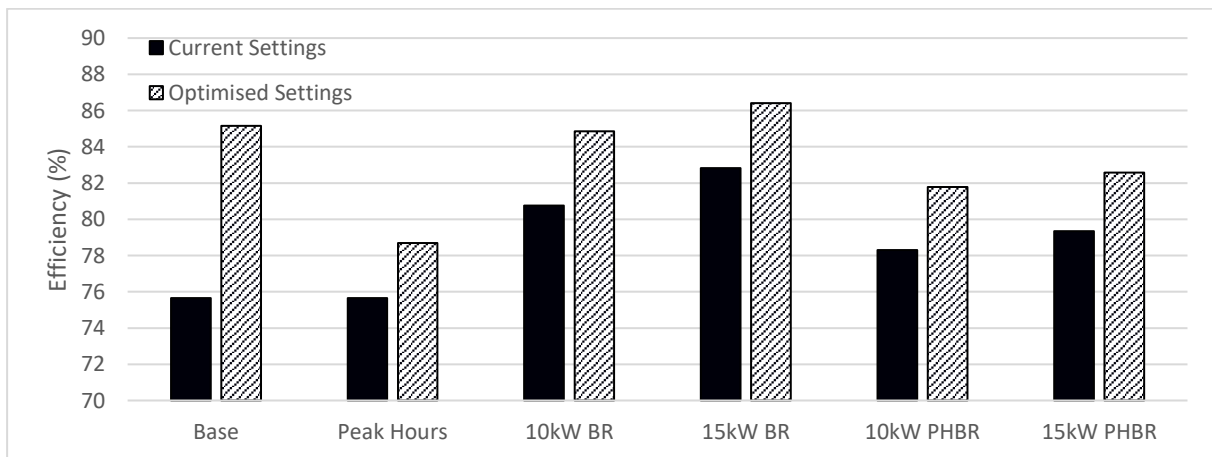

Figure 6: Battery system round trip efficiency

The effect of the limited peak hour grid import is made clear in Fig 7. The prescence of some energy imported during this time is to cover base loads in the case of no EV load to prevent the battery from discharging at extremely low powers, thus maintaining a high round-trip efficiency. For the optimal settings, an imposed battery charge/discharge power requirement results in an increased grid import during peak hours, with respect to both the optimal base case and current settings. The control prioritises battery discharge above the assigned power requirement, therefore, at the end of the day the battery is more depleted with respect to the base case. This is consistent with the P&R usage pattern which tend towards high EV load in the morning and early afternoon due to the prescence of commuters. With optimal grid connection capacity the high battery charging power could fully recharge the battery in the three hour window. Furthermore, the low battery utilisation in the optimal base case means the battery is not often recharged during these peak hours.
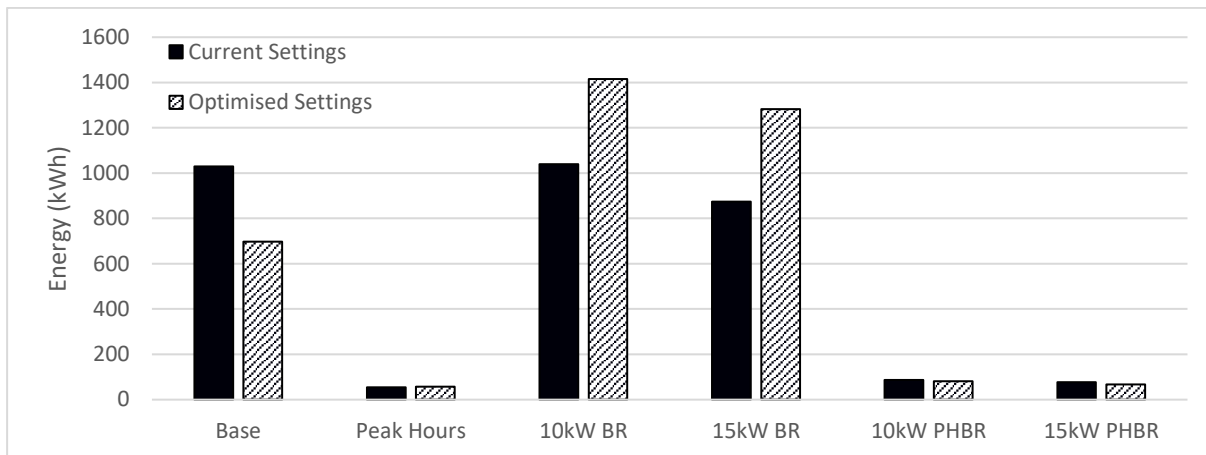
Figure 7: Energy imported from the grid during peak grid load hours

The total load supplied by the battery, displayed in Fig 8, is as expected. By enabling the battery to supply the full load during battery discharge periods, the battery will of course deliver more energy than the base case. Furthermore, having a lower battery discharge requirement enables the battery to supply at lower loads, and therefore more often. This holds true for both current and optimal settings. Similarly, limiting the energy import during peak hours forces the battery to supply the load at times that in the base case it would not, i.e. when the EV load is less than grid capacity.
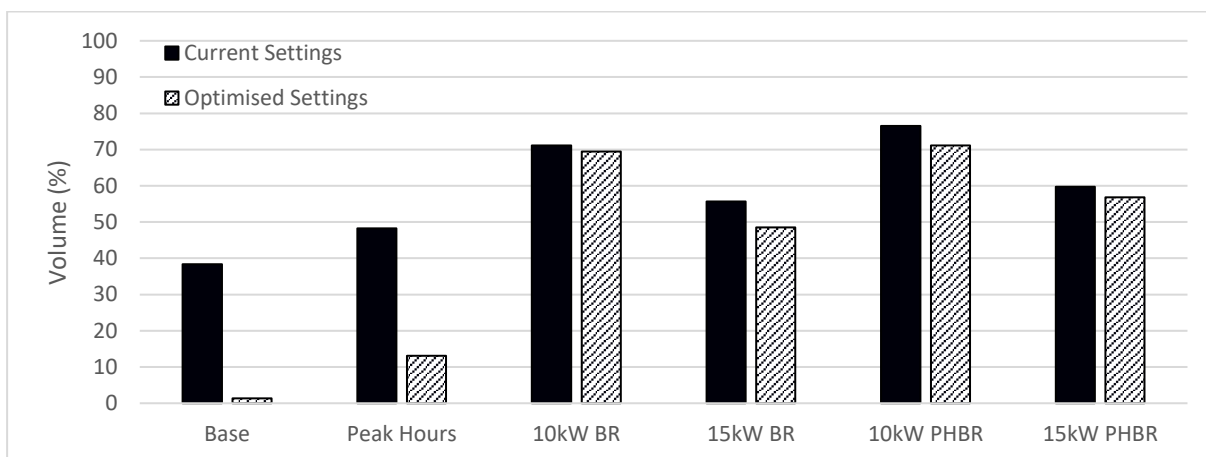

Figure 8: Total load supplied by the battery

The number of users that end the charging session when the vehicle is still being charged is higher in all scenarios than the base case for both current and optimal system settings, as can be seen in Fig 9. This suggests that the charge session is incomplete, in so far as the car could have received more energy. In these cases, more energy can only be supplied to the user if there is enough available capacity. As shown in Fig 5, the optimal system sizing suffers from less loss of load, meaning less times of insufficient capacity. Therefore, having a high grid connection capacity tends to be able to deliver more energy and therefore generate higher revenue.
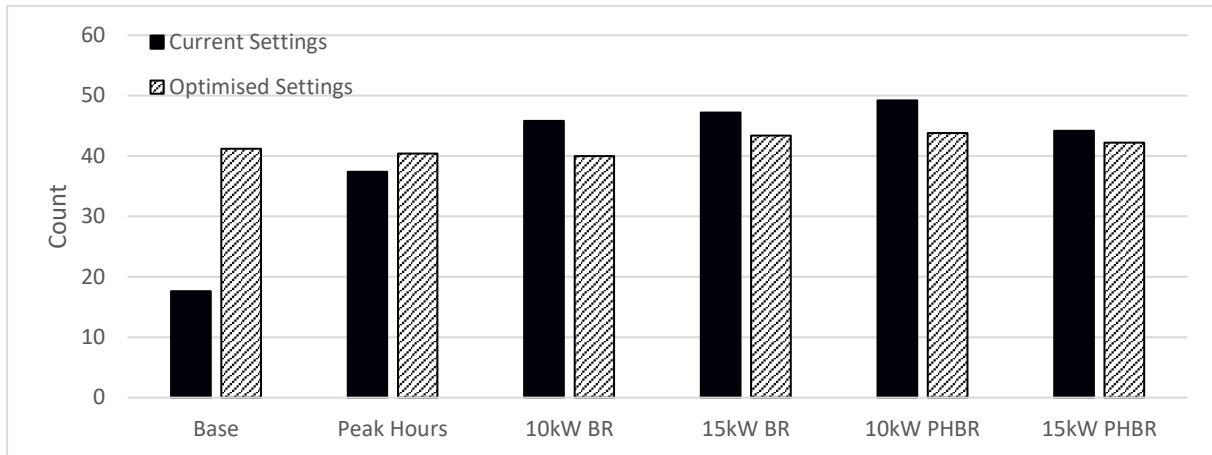
Figure 9: Users still charging at the time of disconnection, suggesting incomplete charging

The control strategies investigated generally perform better when using the optimal sizing than the current system sizing for the frequently observed 5 MWh monlthy load. When the monthly load increases the disparity between optimal sizing and current sizing system performance will increase. This is made clear in Tab 5 where the loss of potential load was only 7 kWh for the optimal sizing and over 700 kWh for the current sizing, when using the base case control. Assuming the patterns observed in Fig 5 remain valid, other control strategies will only result in higher lost load.

With a lost load of approximately 1%, high battery round-trip efficiency of 85 %, and highly utilised battery, the 10 kW BR control is deemed the best control when using the optimal system sizing. However, this does result in high peak hour grid energy import. The maximum power drawn is of course the grid connection capacity, 55 kW. This is equal across all control strategies, so the increased power demand on the AC grid and the local substation is no higher, though it will inevitably be for a longer duration.

The control method used when performing the iterative optimisation process undoubtedly has a large effect. For instance, if the system was optimised using the 15 kW PHBR control strategy the battery would inevitably require a larger energy storage capacity to satisfy constraint 7, the amount of potential load lost. Therefore, for a more comprehensive and accurate recommendation of correct sizing and control strategy many more optimisation processes would need to be completed. Furthermore, these are only a handful of specific, yet limited, control strategies that are intended to address specific performance metrics and are not exhaustive. There will be another, better suited control strategy that could be employed for this use case. Thus, further study would be required.

Finally, if the battery were to be used for grid ancillary services, such as frequency response and voltage control, then an additional revenue would be available for the battery and the optimisation objective function would be reformed. In this case the optimal sizing would be different, likely tending towards a larger battery to benefit from ancillary service revenue whilst still maintaining security of supply for the P&R users.

4   Conclusion

With the use of data from a battery supported EV charging plaza with a limited capacity grid connection a validated stochastic system model was developed. The model was used to optimise both the battery energy storage capacity and grid connection capacity for the future proof monthly load profile of 7 MWh. Finally, using the optimal system sizing a variety of control strategies were simulated for the commonly observed 5 MWh monthly load. The results were compared to simulations using the current system sizing for the same control strategies. The control strategies investigated were the limitation of grid energy import during peak grid load hours, the implementation of a minimum required battery charging and discharging power, and a combination of the two.

The optimal battery sizing was determined to be 143 kWh and 103 kW with a grid connection capacity of 3x80 A (55.4 kW), compared to the currently used 3x25 A (17.3 kW) grid connection and a battery size of 336 kWh and 240 kW. This implies that the current battery is significantly oversized and that the grid connection could be increased. The proposed method provides an opportunity to calculcate optimal system

dimensions given a certain load profile beforehand to avoid unnecessary investment costs. The recommended control strategy, considering the optimal sizing, common monthly load of 5 MWh, and desirable performance metrics, namely high roundtrip efficiency, smarter battery cycling, and minimal peak grid load hour import, was found to be the implementation of a 10 kW requirement for battery charging and discharging.

Acknowledgments

References

[1] Nationale Agenda Laadinfrastructure, *The National Charging Infrastructure Agenda,* Technical Report, Ministry of Infrastructure and Water Management 2021

[2] Over Morgen & Gemeente Amsterdam, *Transitievisie Warmte Amsterdam*, Technical Report, 2020

[3] Gemeente Amsterdam, *Laad me: Strategisch plan Laadinfrastructuur 2020 – 2030*, Techincal Report 2020

[4] Netherlands Enterprise Agency, *Electric Vehicles Statistics in the Netherlands: Up to and including January 2023*, Technical Report, 2023

[5] Liander, https://www.liander.nl/grootzakelijk/aansluiting/nieuw, accessed 13/03/2023

[6] Liander, *Tarieven voor aansluiting en transport elektriciteit*: *Voor huishoudens en zakelijke klanten met een kleinverbruikaansluiting per 1 januari*, Technical Report, 2023

[7] J. Blank, & K. Deb, *Pymoo: Multi-objective optimization in python. IEEE Access*, *8*, 89497-89509, 2020

[8] Ralon, P., Taylor, M., Ilas, A., Diaz-Bone, H., & Kairies, K. (2017). Electricity storage and renewables: Costs and markets to 2030. *International Renewable Energy Agency: Abu Dhabi, United Arab Emirates*, *164*.

[9] Stecca, M., Soeiro, T. B., Elizondo, L. R., Bauer, P., & Palensky, P. (2021). Lifetime estimation of grid-connected battery storage and power electronics inverter providing primary frequency regulation. *IEEE Open Journal of the Industrial Electronics Society*, *2*, 240-251.

[10] Andrenacci, N., Chiodo, E., Lauria, D., & Mottola, F. (2018). Life cycle estimation of battery energy storage systems for primary frequency regulation. *Energies*, *11*(12), 3320.

Presenter Biography

Edward holds a MSc degree from the Technical University of Delft, the Netherlands, and has been conducting research in the e-mobility sector at the Amsterdam University of Applied Sciences since 2021. His research thus far has included energy modelling and grid integration of electric vehicles.